Long-range interaction and nonlinear localized modes in photonic crystal waveguides

Serge F. Mingaleev,[1,][*] Yuri S. Kivshar,[1] and Rowland A. Sammut[2]

[1]*Optical Sciences Centre, Australian National University, Canberra ACT 0200, Australia*
[2]*School of Mathematics and Statistics, Australian Defence Force Academy, Canberra ACT 2600, Australia*

We develop the theory of nonlinear localized modes (intrinsic localized modes or discrete breathers) in two-dimensional (2D) photonic crystal waveguides. We consider different geometries of the waveguides created by an array of nonlinear dielectric rods embedded into an otherwise perfect linear 2D photonic crystal, and demonstrate that the effective interaction in such waveguides is nonlocal, being described by a nonlinear lattice model with long-range coupling and nonlocal nonlinearity. We reveal the existence of different types of nonlinear guided mode that are also localized in the waveguide direction, and describe their unique properties, including bistability.

PACS number(s): 42.70.Qs, 42.79.Gn, 42.65.Wi, 42.65.Tg

I. INTRODUCTION

In physics, the idea of localization is generally associated with disorder that breaks translational invariance. However, research in recent years has demonstrated that localization can occur in the absence of any disorder and solely due to nonlinearity, in the form of *intrinsic localized modes*, also called *discrete breathers* [1]. A rigorous proof of the existence of time-periodic, spatially localized solutions describing such nonlinear modes has been presented for a broad class of Hamiltonian coupled-oscillator nonlinear lattices [2], but approximate analytical solutions can also be found in many other cases, demonstrating the generality of the concept of nonlinear localized modes.

Nonlinear localized modes can be easily identified in numerical molecular-dynamics simulations in many different physical models (see, e.g., Ref. [1] for a review), but only very recently have the first experimental observations of spatially localized nonlinear modes been reported in mixed-valence transition metal complexes [3], quasi-one-dimensional antiferromagnetic chains [4], and arrays of Josephson junctions [5]. Importantly, very similar types of spatially localized nonlinear modes have been experimentally observed in macroscopic mechanical [6] and guided-wave optical [7] systems.

Recent experimental observations of nonlinear localized modes, as well as numerous theoretical results, indicate that both effects, i.e., nonlinearity-induced localization and spatially localized modes, can be expected in physical systems of very different nature. From the viewpoint of possible practical applications, self-localized states in optics seem to be the most promising ones; they can lead to different types of nonlinear all-optical switching devices where light manipulates and controls light itself, by varying the input intensity. As a result, the study of nonlinear localized modes in photonic structures is expected to lead to a variety of realistic applications of intrinsic localized modes.

One of the promising fields where the concept of nonlinear localized modes may find practical applications is in the physics of *photonic crystals* [or photonic band gap (PBG) materials]—periodic dielectric structures that produce many of the same phenomena for photons as does the crystalline atomic potential for electrons [8]. Three-dimensional (3D) photonic crystals for visible light have been successfully fabricated only within the past year or two, and presently many research groups are working on creating tunable band-gap switches and transistors operating entirely with light. The most recent idea is to employ nonlinear properties of band-gap materials, thus creating nonlinear photonic crystals that have 2D or 3D periodic nonlinear susceptibility [9,10].

Nonlinear photonic crystals or photonic crystals with embedded nonlinear impurities create an ideal environment for the generation and observation of nonlinear localized photonic modes. In particular, the existence of such modes for the frequencies in the photonic band gaps has been predicted [11] for 2D and 3D photonic crystals with Kerr nonlinearity. Nonlinear localized modes can also be excited at nonlinear interfaces with quadratic nonlinearity [12], or along dielectric waveguide structures possessing a nonlinear Kerr-type response [13]. In this paper, we analyze nonlinear localized modes in 2D photonic crystal waveguides. We consider the waveguides created by an array of dielectric rods embedded into an otherwise perfect 2D photonic crystal. It is assumed that the dielectric constant of the waveguide rods depends on the field intensity (due to the Kerr effect), so that waveguides of different geometries can support a variety of nonlinear guided modes. We demonstrate here that localization can occur in the propagation direction creating a 2D spatially localized mode (see Fig. 9 below). As follows from our results, the effective interaction in such nonlinear waveguides is nonlocal, and the nonlinear localized modes are described by a nontrivial generalization of nonlinear lattice models with long-range coupling and nonlocal nonlinearity.

II. MODEL

We consider a 2D photonic crystal created by a square lattice of parallel, infinitely long dielectric columns (or rods) in air. The rods are assumed to be parallel to the x_3 axis, so that the system is characterized by the dielectric constant $\epsilon(\boldsymbol{x}) = \epsilon(x_1, x_2)$. The evolution of the E-polarized light [with the electric field having the structure $\boldsymbol{E} = (0,0,E)$], propagat-

---

*On leave from the Bogolyubov Institute for Theoretical Physics, 14-b Metrologichna Str., Kiev 03143, Ukraine.
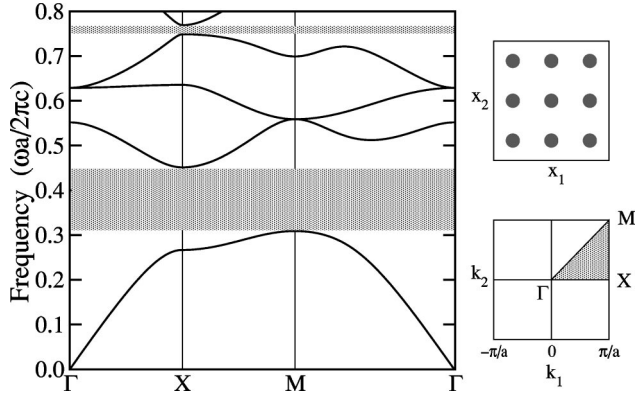
FIG. 1. The band-gap structure of the photonic crystal consisting of a square lattice of dielectric rods with $r_0=0.18a$ and $\epsilon_0=11.56$ (the band gaps are shaded gray). The top right inset shows a cross-sectional view of the 2D photonic crystal. The bottom right inset shows the corresponding Brillouin zone, with the irreducible zone shaded gray.

ing in the (x_1,x_2) plane, is governed by the scalar wave equation

$$\nabla^2 E(\boldsymbol{x},t)-\frac{1}{c^2}\partial_t^2[\epsilon(\boldsymbol{x})E]=0, \tag{1}$$

where $\nabla^2\equiv\partial_{x_1}^2+\partial_{x_2}^2$. For monochromatic light, we consider the stationary solutions

$$E(\boldsymbol{x},t)=e^{-i\omega t}E(\boldsymbol{x}|\omega),$$

and the equation of motion (1) reduces to the simple eigenvalue problem

$$\left[\nabla^2+\left(\frac{\omega}{c}\right)^2\epsilon(\boldsymbol{x})\right]E(\boldsymbol{x}|\omega)=0. \tag{2}$$

This eigenvalue problem can be solved, e.g., by the plane wave method [14], in the case of a perfect photonic crystal, for which the dielectric constant $\epsilon(\boldsymbol{x})\equiv\epsilon_{pc}(\boldsymbol{x})$ is a periodic function

$$\epsilon_{pc}(\boldsymbol{x}+\boldsymbol{s}_{ij})=\epsilon_{pc}(\boldsymbol{x}), \tag{3}$$

where i and j are arbitrary integers and

$$\boldsymbol{s}_{ij}=i\boldsymbol{a}_1+j\boldsymbol{a}_2 \tag{4}$$

is a linear combination of the primitive lattice vectors $\boldsymbol{a}_1$ and $\boldsymbol{a}_2$ of the 2D photonic crystal.

For definiteness, we consider the 2D photonic crystal earlier analyzed (in the linear limit) in Refs. [15,16], i.e., we assume that the rods are identical and cylindrical, with radius $r_0=0.18a$ and dielectric constant $\epsilon_0=11.56$. The rods form a perfect square lattice with the distance a between two neighboring rods, i.e. $\boldsymbol{a}_1=a\boldsymbol{x}_1$ and $\boldsymbol{a}_2=a\boldsymbol{x}_2$. The frequency band structure for this type of 2D photonic crystal, and for the selected polarization of the electric field, is shown in Fig. 1. As follows from the structure of the frequency spectrum, there exists a large (38%) band gap that extends from the lower cutoff frequency $\omega=0.302\times2\pi c/a$ to the upper band-gap frequency $\omega=0.443\times2\pi c/a$. Since the characteristics of a PBG material remain unchanged under rescaling, we can assume that this gap is created in either the infrared or visible

region of the spectrum. For example, if we choose the lattice constant to be $a=0.58$ μm, the wavelength corresponding to the mid-gap frequency will be 1.55 μm.

The light cannot propagate through the photonic crystal if its frequency falls inside the band gap. But one can excite guided modes inside the forbidden frequency gap by introducing some interfaces, waveguides, or defects. Here, we consider waveguides created by a row of identical defects with a Kerr-type nonlinear response. These defect-induced waveguides possess translational symmetry, and the corresponding guided modes can be characterized by the reciprocal space wave vector k directed along the waveguide. Such a guided mode has a periodical profile along the waveguide, and it decays exponentially in the transverse direction.

Linear photonic crystal waveguides created by removing a row of dielectric rods have been recently investigated numerically [15,16] and experimentally [17]. In particular, highly efficient transmission of light, even in the case of a bent waveguide, has been demonstrated.

In the present paper, in contrast to Refs. [15–17] where only linear waveguides were considered, we study the properties of nonlinear waveguides created by inserting an additional row of rods fabricated from a Kerr-type nonlinear material characterized by the third-order nonlinear susceptibility with the linear dielectric constant ϵ_d. For definiteness, we assume that $\epsilon_d=\epsilon_0=11.56$. As we show below, by changing the radius r_d of these defect rods and their location within the crystal, we can create waveguides with quite different properties.

III. EFFECTIVE DISCRETE EQUATIONS

Writing the dielectric constant $\epsilon(\boldsymbol{x})$ as a sum of periodic and defect-induced terms, i.e.,

$$\epsilon(\boldsymbol{x})=\epsilon_{pc}(\boldsymbol{x})+\delta\epsilon(\boldsymbol{x}|E),$$

we can present Eq. (2) as follows:

$$\left[\nabla^2+\left(\frac{\omega}{c}\right)^2\epsilon_{pc}(\boldsymbol{x})\right]E(\boldsymbol{x}|\omega)=-\left(\frac{\omega}{c}\right)^2\delta\epsilon(\boldsymbol{x}|E)E(\boldsymbol{x}|\omega). \tag{5}$$

Equation (5) can also be written in the integral form

$$E(\boldsymbol{x}|\omega)=\left(\frac{\omega}{c}\right)^2\int d^2\boldsymbol{y}\,G(\boldsymbol{x},\boldsymbol{y}|\omega)\,\delta\epsilon(\boldsymbol{y}|E)E(\boldsymbol{y}|\omega), \tag{6}$$

where $G(\boldsymbol{x},\boldsymbol{y}|\omega)$ is the Green function, which is defined, in a standard way, as a solution of the equation

$$\left[\nabla^2+\left(\frac{\omega}{c}\right)^2\epsilon_{pc}(\boldsymbol{x})\right]G(\boldsymbol{x},\boldsymbol{y}|\omega)=-\delta(\boldsymbol{x}-\boldsymbol{y}),$$

with, according to Eq. (3), periodic coefficients. The properties of the Green function and the numerical methods for its calculation have already been described in the literature [14,18]. Here, we notice that the Green function of a perfect 2D photonic crystal is *symmetric*, i.e.,

$$G(\boldsymbol{x},\boldsymbol{y}|\omega)=G(\boldsymbol{y},\boldsymbol{x}|\omega)$$

and *periodic*, i.e.,

$$G(\boldsymbol{x}+\boldsymbol{s}_{ij},\boldsymbol{y}+\boldsymbol{s}_{ij}|\omega)=G(\boldsymbol{x},\boldsymbol{y}|\omega),$$

where s_{ij} is defined by Eq. (4).

Let us consider a row of nonlinear defect rods embedded into the crystal along a selected direction. To describe such a row, we should define the rods positions along s_{ij} with some specific values of i and j. For example, let us first assume that the defect rods are located at the points $x_m = x_0 + m s_{ij}$. In this case, the correction to the dielectric constant is

$$\delta\epsilon(x) = [\epsilon_d + |E(x|\omega)|^2] \sum_m \theta(x - x_m), \qquad (7)$$

where

$$\theta(x) = \begin{cases} 1 & \text{for } |x| \leq r_d \\ 0 & \text{for } |x| > r_d. \end{cases}$$

The parameter ϵ_d in Eq. (7) is the dielectric constant of the defect rods in the linear limit, while the second term takes into account a contribution due to the Kerr nonlinearity (the electric field is scaled with the coefficient of nonlinear susceptibility $\chi^{(3)}$). The radius of the rods r_d is assumed to be sufficiently small so that the electric field $E(x|\omega)$ is almost constant inside the defect rods. We substitute Eq. (7) into Eq. (6) and, averaging over the cross section of the rods, derive an approximate *discrete nonlinear equation* for the electric field,

$$E_n = \sum_m J_{n-m}(\omega)(\epsilon_d + |E_m|^2)E_m, \qquad (8)$$

where

$$J_n(\omega) = \left(\frac{\omega}{c}\right)^2 \int_{r_d} d^2y \, G(x_0, x_n + y|\omega). \qquad (9)$$

This type of discrete nonlinear equation for photonic crystals was earlier introduced by McGurn [13], for the special case of nonlinear impurities embedded in linear rods. However, the analytical approach developed by McGurn for that model did not take into account the field distribution via the explicit dependence of the coupling coefficients $J_n(\omega)$ and, as a result, Eq. (8) was not solved exactly. Moreover, the analysis of Ref. [13] was based on the nearest-neighbor approximation where the coupling coefficients are approximated as $J_n = J_0 \delta_{n,0} + J_1 \delta_{n,\pm 1}$ with constant J_0 and J_1.

In sharp contrast, in the present paper we provide a systematic analysis of different types of nonlinear localized modes in the framework of a complete model of a 2D photonic crystal. In particular, we reveal that the approximation of the nearest-neighbor interaction is very crude in many of the cases we analyzed. Since the effective coupling coefficients are defined by the Green function, this can be seen directly from Fig. 2, which shows a typical spatial profile of the Green function that, in general, characterizes a long-range interaction, very typical for photonic crystal waveguides. As a consequence of that, the coupling coefficients $|J_n(\omega)|$ calculated from Eq. (9) decrease slowly with the site number n. For some directions, the coupling coefficients can be approximated by an exponential function as follows:

$$|J_n(\omega)| \approx \begin{cases} J_0(\omega) & \text{for } n = 0 \\ J_*(\omega) \, e^{-\alpha(\omega)|n|} & \text{for } |n| \geq 1, \end{cases}$$
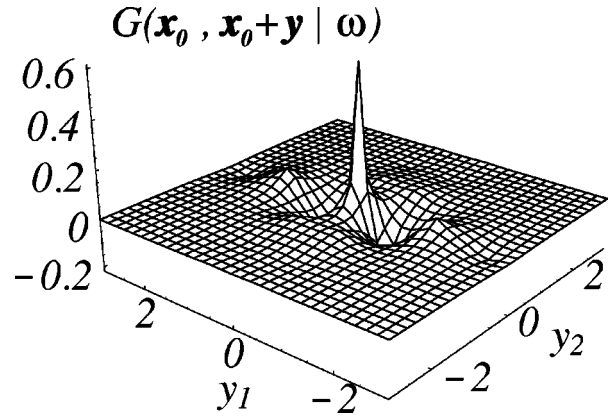

FIG. 2. The Green function $G(x_0, x_0 + y|\omega)$ for $x_0 = a_1/2$ and $\omega = 0.33 \times 2\pi c/a$.

where the characteristic decay rate $\alpha(\omega)$ can be as small as 0.85, depending on the values of ω, x_0, s_{ij}, and r_d, and can be even smaller for other types of photonic crystals.

This result allows us to draw an analogy with a class of the nonlinear Schrödinger (NLS) equations that describe nonlinear excitations in quasi-one-dimensional molecular chains with long-range (e.g., dipole-dipole) interaction between the particles and local on-site nonlinearities [19]. For such systems, it was shown that the effect of nonlocal interparticle interaction introduces some new features into the properties of existence and stability of nonlinear localized modes. Moreover, for our model the coupling coefficients $J_n(\omega)$ can be either nonstaggered and monotonically decaying, i.e., $J_n(\omega) = |J_n(\omega)|$, or staggered and oscillating from site to site, i.e., $J_n(\omega) = (-1)^n |J_n(\omega)|$. We can therefore expect that effective nonlocality in both linear and nonlinear terms of Eq. (8) will cause a number of additional features in the properties of nonlinear localized modes excited in photonic crystal waveguides.

IV. EXAMPLES OF NONLINEAR MODES

As can be seen from the structure of the Green function, presented in Fig. 2, the case of monotonically varying coefficients $J_n(\omega)$ can be obtained for the waveguide oriented in the s_{01} direction with $x_0 = a_1/2$. In this case, the frequency of a linear guided mode that can be excited in such a waveguide takes the minimum value at $k = 0$ (see Fig. 3), and the corresponding nonlinear mode is expected to be nonstaggered.

We have solved Eq. (8) numerically and found that nonlinearity can lead to the existence of a new type of guided mode localized in both directions, i.e., in the direction perpendicular to the waveguide, due to the guiding properties of a channel waveguide created by defect rods, and in the direction of the waveguide, due to the nonlinearity-induced self-trapping effect. Such nonlinear modes exist with frequencies below the frequency of the linear guided mode of the waveguide, i.e., below the frequency ω_A in Fig. 3, and are indeed nonstaggered, with the bell-shaped profile along the waveguide direction shown in the left inset of Fig. 4.

The 2D nonlinear modes localized in both dimensions can be characterized by the mode intensity which we define, by analogy with the NLS equation, as
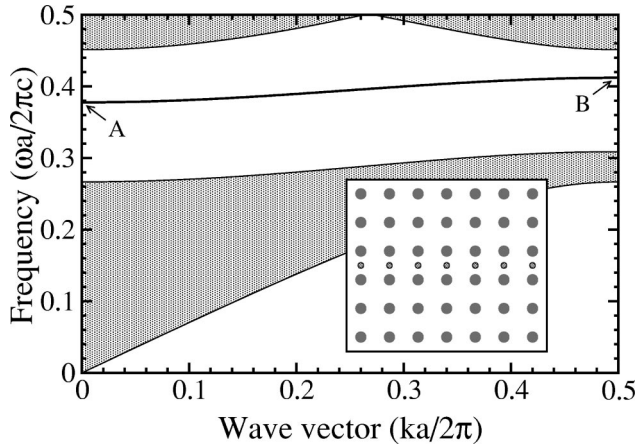
FIG. 3. Dispersion relation for the photonic crystal waveguide shown in the inset ($\epsilon_0 = \epsilon_d = 11.56$, $r_0 = 0.18a$, $r_d = 0.10a$). The gray areas are the projected band structure of the perfect 2D photonic crystal. The frequencies at the indicated points are $\omega_A = 0.378 \times 2\pi c/a$ and $\omega_B = 0.412 \times 2\pi c/a$.

$$Q = \sum_n |E_n|^2. \qquad (10)$$

This intensity is closely related to the energy of the electric field in the 2D photonic crystal accumulated in the nonlinear mode. In Fig. 4 we plot the dependence of Q on frequency, for the waveguide geometry shown in Fig. 3.

As can be seen from the example of the Green function shown in Fig. 2, the case of staggered coupling coefficients $J_n(\omega)$ can be obtained for a waveguide oriented in the s_{10} direction with $x_0 = a_1/2$. In this case, the frequency dependence of the linear guided mode of the waveguide takes the minimum at $k = \pi/a$ (see Fig. 5). Accordingly, a nonlinear guided mode localized along the direction of the waveguide is expected to exist with frequency below the lowest frequency ω_A of the linear guided mode, with a staggered profile. The longitudinal profile of such a 2D nonlinear localized mode is shown in the left inset in Fig. 6, together with the dependence of the mode intensity Q on the frequency (solid curve), which in this case is again monotonic. It should be

FIG. 5. Dispersion relation for the photonic crystal waveguide shown in the inset ($\epsilon_0 = \epsilon_d = 11.56$, $r_0 = 0.18a$, $r_d = 0.10a$). The gray areas are the projected band structure of the perfect 2D photonic crystal. The frequencies at the indicated points are $\omega_A = 0.346 \times 2\pi c/a$ and $\omega_B = 0.440 \times 2\pi c/a$.

noted that in addition to the symmetric modes shown in the left inset in Fig. 6 there exist also *antisymmetric localized modes* [13]. However, our calculations show that the intensity of the antisymmetric modes always exceeds that for symmetric ones. Thus, antisymmetric modes are expected to be unstable and should transform into lower-energy symmetric modes.

The results presented above were obtained for linear photonic crystals with nonlinear waveguides created by a row of defect rods. However, we have carried out the same analysis for the general case of a nonlinear photonic crystal that is created by rods of different size but made of the same nonlinear material. Importantly, we have found very small differences from all the results presented above provided nonlinearity is relatively weak. In particular, for the photonic crystal waveguide shown in Fig. 5, the results for linear and nonlinear photonic crystals are very close. Indeed, for the
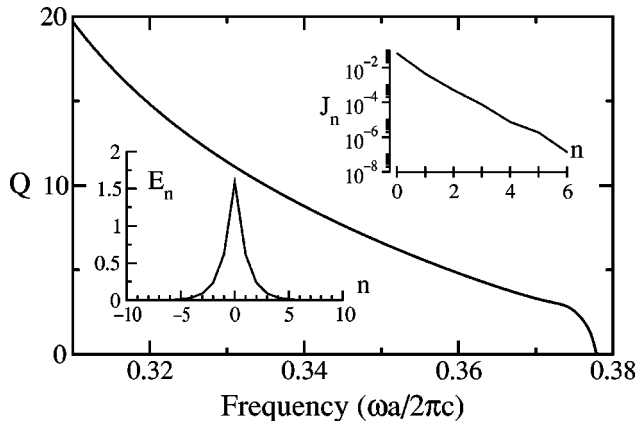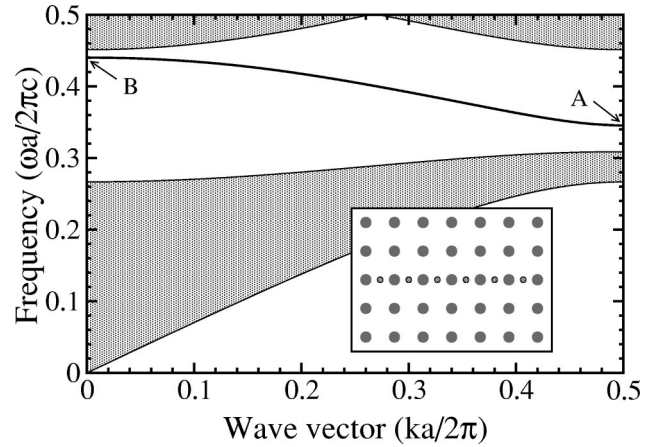

FIG. 4. Intensity $Q(\omega)$ of the nonlinear mode excited in the photonic crystal waveguide shown in Fig. 3. The right inset gives the dependence $J_n(\omega)$ calculated at $\omega = 0.37 \times 2\pi c/a$. The left inset presents the profile of the corresponding nonlinear localized mode.
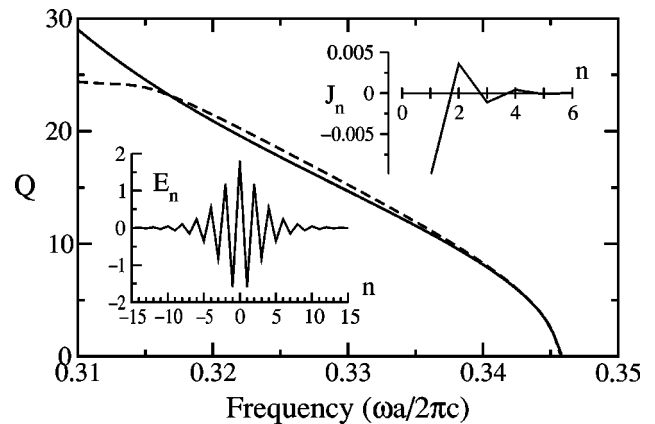

FIG. 6. Intensity $Q(\omega)$ of the nonlinear mode excited in the photonic crystal waveguide shown in Fig. 5. The solid curve corresponds to the case of nonlinear rods in a linear photonic crystal, whereas the dashed curve is the same dependence for the case of a nonlinear photonic crystal. The right inset shows the behavior of the coupling coefficients $J_n(\omega)$ for $n \geq 1$ ($J_0 = 0.045$) at $\omega = 0.33 \times 2\pi c/a$. The left inset shows the profile of the corresponding nonlinear mode.
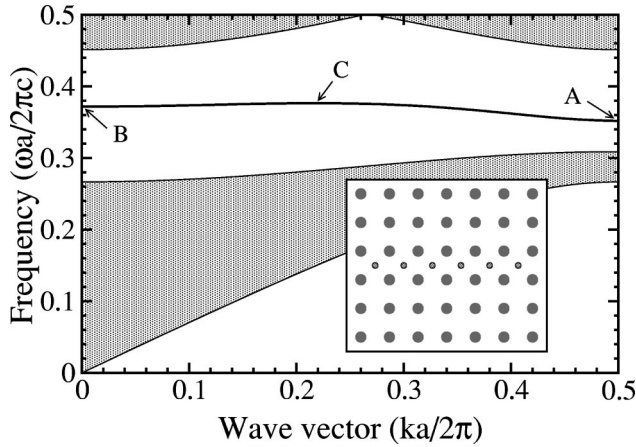
FIG. 7. Dispersion relation for the photonic crystal waveguide shown in the inset ($\epsilon_0 = \epsilon_d = 11.56$, $r_0 = 0.18a$, $r_d = 0.10a$). The gray areas are the projected band structure of the perfect crystal. The frequencies at the points indicated are $\omega_A = 0.352 \times 2\pi c/a$, $\omega_B = 0.371 \times 2\pi c/a$, and $\omega_C = 0.376 \times 2\pi c/a$ (at $k = 0.217 \times 2\pi/a$).

mode intensity Q the results corresponding to a nonlinear photonic crystal are shown in Fig. 6 by a dashed curve, and for $Q < 20$ this curve almost coincides with the solid curve corresponding to the case of a nonlinear waveguide embedded into a 2D linear photonic crystal.

Let us now consider a waveguide created by a row of defects that are located at the points $x_0 = (a_1 + a_2)/2$ along a straight line in either the s_{10} or s_{01} direction. The results for this case are presented in Figs. 7–9. The coupling coefficients $|J_n|$ are described by a slowly decaying function of the site number n, so that the effective interaction decays on scales much larger than those in the two cases considered above. As for NLS models with long-range dispersive interactions [19,20], for this type of nonlinear photonic crystal waveguide we find a nonmonotonic behavior of the mode intensity $Q(\omega)$ and, as a result, multivalued dependence of the invariant $Q(\omega)$ for $\omega < 0.347 \times 2\pi c/a$. Similar to the results earlier obtained for the nonlocal NLS models [19], we
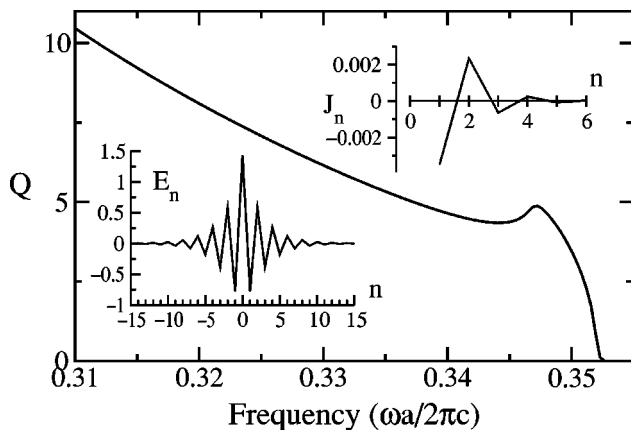

FIG. 8. Intensity $Q(\omega)$ of the nonlinear mode excited in the photonic crystal waveguide shown in Fig. 7. The right inset shows the behavior of the coupling coefficients $J_n(\omega)$ for $n \geq 1$ ($J_0 = 0.068$) at $\omega = 0.345 \times 2\pi c/a$. The left inset shows the profile of the corresponding nonlinear mode.
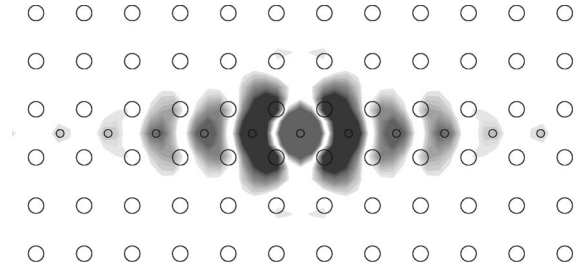

FIG. 9. Electric field of the nonlinear localized mode in a waveguide that corresponds to the longitudinal cross section shown in the left inset of Fig. 8. The rod positions are indicated by circles.

can expect here that nonlinear localized modes corresponding, in our notations, to positive slope of the derivative $dQ/d\omega$ are unstable and will eventually decay or transform into modes of higher or lower frequency [21]. Such a phenomenon is known as *bistability*, and in this problem it occurs as a direct manifestation of the nonlocality of the effective (linear and nonlinear) interaction between the defect rod sites. However, a rigorous analysis of the mode stability is beyond the scope of this paper and will be addressed in future publications.

V. CONCLUSIONS

Exploration of nonlinear properties of PBG materials is an active direction of research, and it may open up a broad class of applications of photonic crystals for all-optical signal processing and switching, allowing an effective way to create tunable band-gap structures operating entirely with light. Nonlinear photonic crystals, and nonlinear waveguides embedded into photonic structures with periodically modulated dielectric constant, create an ideal environment for the generation and observation of nonlinear localized modes.

In the present paper, we have developed a consistent theory of the nonlinear localized modes that can be excited in photonic crystal waveguides of different geometry. For several geometries of 2D waveguide, we have demonstrated that such modes are described by a nonlinear lattice model that includes long-range interaction and effectively nonlocal nonlinear response. It is expected that the general features of nonlinear guided modes described here will be preserved in other types of photonic crystal waveguides. Our approach and results can also be useful to develop the theory of nonlinear two-frequency parametric localized modes in the recently fabricated 2D photonic crystals with second-order nonlinear susceptibility [22]. Additionally, similar types of nonlinear localized modes are expected in photonic crystal fibers [23] consisting of a periodic air-hole lattice that runs along the length of the fiber, provided the fiber core is made of a highly nonlinear material (see, e.g., Ref. [24]).

[1] S. Flach and C. R. Willis, Phys. Rep. **295**, 181 (1998); O. M. Braun and Yu. S. Kivshar, *ibid.* **306**, 1 (1998), Sec. 6.

[2] R. S. MacKay and S. Aubry, Nonlinearity **7**, 1623 (1994); see also S. Aubry, Physica D **103**, 201 (1997).

[3] B. I. Swanson, J. A. Brozik, S. P. Love, G. F. Strouse, A. P. Shreve, A. R. Bishop, W. Z. Wang, and M. I. Salkola, Phys. Rev. Lett. **82**, 3288 (1999).

[4] U. T. Schwarz, L. Q. English, and A. J. Sievers, Phys. Rev. Lett. **83**, 223 (1999).

[5] E. Trias, J. J. Mazo, and T. P. Orlando, Phys. Rev. Lett. **84**, 741 (2000); P. Binder, D. Abraimov, A. V. Ustinov, S. Flach, and Y. Zolotaryuk, *ibid.* **84**, 745 (2000).

[6] F. M. Russel, Y. Zolotaryuk, and J. C. Eilbeck, Phys. Rev. B **55**, 6304 (1997).

[7] H. S. Eisenberg, Y. Silberberg, R. Marandotti, A. R. Boyd, and J. S. Aitchison, Phys. Rev. Lett. **81**, 3383 (1998).

[8] J. D. Joannopoulos, R. D. Meade, and J. N. Winn, *Photonic Crystals: Molding the Flow of Light* (Princeton University Press, Princeton, 1995).

[9] V. Berger, Phys. Rev. Lett. **81**, 4136 (1998).

[10] A. A. Sukhorukov, Yu. S. Kivshar, O. Bang, J. Martorell, J. Trull, and R. Vilaseca, Opt. Photonics News **10**, 34 (1999).

[11] S. John and N. Aközbek, Phys. Rev. Lett. **71**, 1168 (1993); Phys. Rev. E **57**, 2287 (1998).

[12] A. A. Sukhorukov, Yu. S. Kivshar, and O. Bang, Phys. Rev. E **60**, R41 (1999).

[13] A. R. McGurn, Phys. Lett. A **251**, 322 (1999); **260**, 314 (1999).

[14] A. A. Maradudin and A. R. McGurn, in *Photonic Band Gaps and Localization*, Vol. 308 of *NATO Advanced Study Institute, Series B: Physics*, edited by C. M. Soukoulis (Plenum Press, New York, 1993), pp. 247–268.

[15] A. Mekis, J. C. Chen, I. Kurland, S. Fan, P. R. Villeneuve, and J. D. Joannopoulos, Phys. Rev. Lett. **77**, 3787 (1996).

[16] A. Mekis, S. Fan, and J. D. Joannopoulos, Phys. Rev. B **58**, 4809 (1998).

[17] S.-Y. Lin, E. Chow, V. Hietala, P. R. Villeneuve, and J. D. Joannopoulos, Science **282**, 274 (1998).

[18] A. J. Ward and J. B. Pendry, Phys. Rev. B **58**, 7252 (1998).

[19] M. Johansson, Y. B. Gaididei, P. L. Christiansen, and K. Ø. Rasmussen, Phys. Rev. E **57**, 4739 (1998).

[20] Y. B. Gaididei, S. F. Mingaleev, P. L. Christiansen, and K. Ø. Rasmussen, Phys. Rev. E **55**, 6141 (1997).

[21] See, e.g., the examples for continuous generalized NLS models given by D. E. Pelinovsky, V. V. Afanasjev, and Yu. S. Kivshar, Phys. Rev. E **53**, 1940 (1996).

[22] N. G. R. Broderick, G. W. Ross, H. L. Offerhaus, D. J. Richardson, and D. C. Hanna, Phys. Rev. Lett. **84**, 4345 (2000).

[23] T. A. Birks, J. C. Knight, and P. St. J. Russell, Opt. Lett. **22**, 961 (1997).

[24] B. J. Eggleton, P. S. Westbrook, R. S. Windeler, S. Spälter, and T. A. Strasser, Opt. Lett. **24**, 1460 (1999).